

# Analysis of the CFO Successive Interference Cancellation for the OFDMA Uplink

Gustavo J. González<sup>1</sup> · Fernando H. Gregorio<sup>1</sup> ·  
Juan E. Cousseau<sup>1</sup> · Carlos H. Muravchik<sup>2</sup>

Published online: 21 July 2016  
© Springer Science+Business Media New York 2016

**Abstract** The uplink of orthogonal frequency division multiple access or single-carrier frequency division multiple access suffers multiple access interference when carrier frequency offset (CFO) is not properly estimated and compensated. In particular, multicarrier uplink CFO compensation is highly complex due to the multiuser context. Successive interference cancellation algorithms are effectively employed to compensate for the CFO, where the interference produced by each user is handled sequentially through a series of iterations. The main contribution of this work is the analysis of the CFO compensation performance of efficient successive cancellation algorithms. We study the mean square symbol error, and derive a useful upper-bound of the compensation technique performance at convergence. This result extends the general convergence results for the space-alternating generalized expectation-maximization algorithm in the CFO compensation scenario. Finally, we validate the analysis with numerical simulations.

**Keywords** OFDMA · SC-FDMA · CFO compensation · Multiple access interference

---

✉ Gustavo J. González  
ggonzalez@uns.edu.ar

Fernando H. Gregorio  
fernando.gregorio@uns.edu.ar

Juan E. Cousseau  
jcousseau@uns.edu.ar

Carlos H. Muravchik  
carlosm@ing.unlp.edu.ar

<sup>1</sup> CONICET-Department of Electrical and Computer Engineering, Universidad Nacional del Sur, Av. Alem 1253, 8000 Bahía Blanca, Argentina

<sup>2</sup> Laboratorio de Electronica Industrial, Control e Instrumentación (LEICI), Dto. Electrotecnia, Facultad de Ingeniería, UNLP, CC 91, 1900 La Plata, Argentina

## 1 Introduction

Multicarrier techniques, either orthogonal frequency division multiple access (OFDMA) or single carrier frequency division multiple access (SC-FDMA), are efficient uplink schemes for new wireless systems due to their high data throughput, spectral efficiency and versatility [1, 2]. As opposed to the downlink of multicarrier modulation schemes, the high sensitivity to frequency synchronization errors in the uplink of multicarrier access techniques produces multiple access interference (MAI). Specifically, the carrier frequency offset (CFO) between each transmitter and the receiver destroys the orthogonality among subcarriers leading to MAI between users. As a consequence, unlike downlink synchronization, uplink synchronization is more challenging because each user is characterized by its own particular CFO and channel parameters [3]. To simplify uplink synchronization, the task is usually divided in a two-step procedure: (1) CFO estimation, and (2) CFO compensation. CFO estimation usually relies on a repetitive structure of special symbols, inserted at the beginning of the frame [3]. In this work we assume that an estimate of the CFO of each user is available [3–5].

Since the CFO affects OFDMA and SC-FDMA in a similar way, a compensation algorithm derived for one modulation can be easily reformulated for the other. A time domain canceler is proposed in [6]. Alternatively, low complexity iterative cancelers based on the Newton's algorithm and the conjugate gradient algorithm were proposed in [7] and [8], respectively. On the other hand, in order to take advantage of the interference structure, the space-alternating generalized expectation-maximization (SAGE) approach [9] is employed in [10] to compensate for the CFO. The SAGE algorithm is an evolution of the expectation-maximization (EM) algorithm [11], where the parameters to be estimated are updated sequentially to facilitate the expectation step and to improve the convergence rate. Beyond the convergence analysis for the conjugate gradient and the Newton's methods, or the general convergence properties of the SAGE algorithm, a convergence analysis for efficient successive cancellation is not available in the literature.

The main contribution of this paper is the analysis of the CFO compensation performance for successive CFO-interference cancellation algorithms. First, we derive an expression of the interference compensation performance in terms of the mean square symbol error of each user, as a function of the number of iterations. From that expression, we obtain a useful analytic upper-bound for the mean square symbol error at convergence. This work completes the analysis and validation of the algorithm presented in [10] and complements the general convergence properties of the SAGE algorithm. To present our analysis, we apply a common multicarrier system framework that models both OFDMA and SC-FDMA systems in a single and direct formulation. Finally, the theoretical mean squared error study is validated by means of simulations.

The outline of the work is the following. The unified multicarrier uplink CFO induced model for OFDMA and SC-FDMA, and the iterative compensation criterion are presented in Sect. 2. The mean square symbol error per user and an upper bound for the compensation performance are presented in Sect. 3. In Sect. 4, numerical simulations are included to illustrate the accuracy of the mean square error upper bound. Finally, Sect. 5 concludes the paper.

## 2 CFO Induced Multiple Access Interference Model

In the uplink of centralized systems, the signals of different users are added together at the base station (BS) [12, 13]. The multicarrier symbol has  $N_c$  subcarriers, where  $N_a$  of them are used for data transmission ( $N_a < N_c$ ) and the remaining are virtual subcarriers (VS) located at the edge of the band, i.e.,  $N_{vs} = (N_c - N_a)/2$  with  $(N_c - N_a)$  even. VS avoid frequency leakage to the neighbor bands [13]. Useful subcarriers are divided into  $K$  subchannels, where each subchannel containing  $N_K = N_a/K$  subcarriers corresponds to a different user. Considering the carrier allocation scheme (CAS), each subchannel is composed by an entire number of tiles  $N_t$  of size  $L_t$ , such that  $N_K = N_t L_t$ . The tiles of each user can be contiguous to form a subband or localized CAS (SCAS), equispaced to form an interleaved or distributed CAS (ICAS), or they can follow a more sophisticated rule to form the generalized CAS (GCAS).

A multicarrier block  $\mathbf{y}$  of size  $N_c$  at the BS, after cyclic prefix removal and the discrete Fourier transform (DFT), can be written as

$$\mathbf{y} = \sum_{m=0}^{K-1} \mathbf{y}^{(m)} + \mathbf{z} \tag{1}$$

where  $\mathbf{y}^{(m)} = \mathbf{F}_{N_c} \mathbf{D}^{(m)} \mathbf{F}_{N_c}^H \mathbf{s}^{(m)}$  is the signal received from user  $m$  corrupted by the channel and the CFO,  $\mathbf{F}_N$  is the  $N$ -point DFT matrix with elements  $[\mathbf{F}_N]_{p,q} = \frac{1}{\sqrt{N_c}} e^{-j2\pi pq/N_c}$  for  $0 \leq p, q \leq N_c - 1$ ,  $\mathbf{D}^{(m)} = \text{diag}\{1, e^{j2\pi \xi^{(m)}/N_c}, \dots, e^{j2\pi \xi^{(m)}(N_c-1)/N_c}\}$ ,  $\xi^{(m)}$  is the CFO of user  $m$  normalized to the intercarrier spacing,  $\mathbf{s}^{(m)} = \mathbf{H}^{(m)} \mathbf{x}^{(m)}$ ,  $\mathbf{x}^{(m)}$  is the symbol of user  $m$ ,  $\mathbf{H}^{(m)} = \text{diag}\{H_0^{(m)}, \dots, H_{N_c-1}^{(m)}\}$ ,  $H_n^{(m)}$   $0 \leq n \leq N_c - 1$  is the DFT of the wireless channel between the user  $m$  and the base station at subcarrier  $n$ , and  $\mathbf{z}$  is a vector of additive white Gaussian noise (AWGN) with variance  $\sigma^2$ . We assume a time synchronous system, i.e., that the cyclic prefix is long enough to accommodate the channel impulse response length and timing misalignments [14]. Additionally, we consider that the channel does not vary within a multicarrier block (block fading assumption).

The ideal received signal in frequency domain, i.e., without CFO, is given by  $\mathbf{s} = \sum_{m=0}^{K-1} \mathbf{s}^{(m)}$ . Considering  $\mathbf{s}^{(m)}$ , the signal of each user, we can write

$$\mathbf{s}^{(m)} = \mathbf{\Psi}^{(m)} \mathbf{s} \tag{2}$$

where  $\mathbf{\Psi}^{(m)}$  is a diagonal selection matrix that takes value one in the column  $p$  if the user  $m$  is allocated to the carrier  $p$  and zero otherwise. Finally, replacing (2) in (1) allows to write the received signal as

$$\mathbf{y} = \mathbf{\Phi} \mathbf{s} + \mathbf{z} \tag{3}$$

where  $\mathbf{\Phi} = \sum_{m=0}^{K-1} \mathbf{\Phi}^{(m)} \mathbf{\Psi}^{(m)}$  is the overall interference matrix and  $\mathbf{\Phi}^{(m)} = \mathbf{F}_{N_c} \mathbf{D}^{(m)} \mathbf{F}_{N_c}^H$ .

The definition of  $\mathbf{x}^{(m)}$  is related to the considered multicarrier system, i.e., OFDMA or SC-FDMA. If  $\mathbf{b}^{(m)}$  is the  $N_K$ -vector of the QAM complex symbols sent by user  $m$  in one multicarrier block, and  $\mathbf{Y}^{(m)}$  is a  $N_c \times N_K$  matrix that takes only the non-zero columns of  $\mathbf{\Psi}^{(m)}$ , i.e.,  $[\mathbf{Y}^{(m)}]_{p,q} = [\mathbf{\Psi}^{(m)}]_{p,q}$  for  $0 \leq p \leq N_c - 1$  and  $q$  is allocated to user ( $m$ ); we can define  $\mathbf{x}^{(m)}$  for OFDMA as  $\mathbf{x}_{ofdma}^{(m)} = \mathbf{Y}^{(m)} \mathbf{b}^{(m)}$  whereas for SC-FDMA is  $\mathbf{x}_{sc-fdma}^{(m)} = \mathbf{Y}^{(m)} \mathbf{F}_{N_K} \mathbf{b}^{(m)}$ .

To compensate for CFO effects in the received multiuser block, we need to obtain an estimate of  $\mathbf{s}$ , denoted  $\hat{\mathbf{s}}$ , from (3). Two estimation criteria can be considered: least squares (LS) and minimum mean squared error (MMSE) [15]. However, we consider only LS since for the SNR range of interest it has the same performance than MMSE with less complexity. LS compensation is given by

$$\hat{\mathbf{s}} = (\Phi^H \Phi)^{-1} \Phi^H \mathbf{y} = \Phi^{-1} \mathbf{y} \tag{4}$$

where the right hand side of this equation is valid only if  $|\zeta^{(m)}| < 0.5$ , i.e. if  $\Phi$  is a full rank, square matrix [15].

In addition, from (4) we can define the compensated symbols of each user as

$$\hat{\mathbf{s}}^{(m)} = \Psi^{(m)} \hat{\mathbf{s}} \tag{5}$$

After CFO compensation, the estimated symbol  $\hat{\mathbf{b}}^{(m)}$  of user  $m$  for the OFDMA system can be obtained from  $\hat{\mathbf{b}}_{ofdma}^{(m)} = (\Upsilon^{(m)})^T (\mathbf{H}^{(m)})^{-1} \hat{\mathbf{s}}$  whereas for the SC-FDMA case it results  $\hat{\mathbf{b}}_{sc-fdma}^{(m)} = \mathbf{F}_{N_k}^H (\Upsilon^{(m)})^T (\mathbf{H}^{(m)})^{-1} \hat{\mathbf{s}}$ . These methods from now on are called *direct compensation*.

Since direct compensation requires the inversion of the interference matrix in (4), the compensation results in a high computational burden. In [10], a successive interference cancellation algorithm that takes into account the interference structure to reduce the complexity is derived. This structure is interesting since it allows to perform a joint CFO estimation and compensation. However, the performance and convergence properties of algorithm are not well explored. After describing the compensation criterion in the next subsection, we analyze the MSE behavior in Sect. 3.

### 2.1 Successive CFO Compensation Criterion

The successive CFO compensation criterion [10] takes advantage of the structure of the interference matrix  $\Phi$ , defined in Sect. 2. The proposal is a formulation of the SAGE algorithm to compensate for the CFO, where the interference is suppressed iteratively by addressing the user’s induced interference sequentially in each iteration. Considering the user  $m$ , the interference is suppressed in two stages: (1) the MAI (i.e., the interference of users  $\{0 \dots m - 1 \ m + 1 \dots K - 1\}$  over user  $m$ ) is canceled, and (2) self-interference of user  $m$  is compensated.

The first step is based on the fact that the contribution of the signal of each user is added at the BS. As  $\mathbf{s}^{(l)}$  for  $l \in \{0, \dots, m - 1, m + 1, \dots, K - 1\}$  are not available at the receiver, they are replaced by previous estimates that will be updated iteratively as in the following expression

$$\hat{\mathbf{y}}_i^{(m)} = \mathbf{y} - \Phi \left( \sum_{l=0}^{m-1} \hat{\mathbf{s}}_{i+1}^{(l)} + \sum_{l=m+1}^{K-1} \hat{\mathbf{s}}_i^{(l)} \right) \tag{6}$$

where  $\hat{\mathbf{y}}_i^{(m)}$  is an estimate of the received signal from user  $m$  at iteration  $i$ ,  $\mathbf{y}$  is the complete received signal,  $\Phi$  is the overall interference matrix, and  $\hat{\mathbf{s}}_i^{(l)}$  are the symbol estimates of user  $l$  at iteration  $i$ . Note that the symbols of users  $\{0, \dots, m - 1\}$  are already updated whereas those of users  $\{m + 1, \dots, K - 1\}$  correspond to the previous iteration.

In the second step, the MAI is assumed already compensated. Following LS for user  $m$  and considering  $\Psi^{(m)}$ , the update equation results

$$\hat{\mathbf{s}}_{i+1}^{(m)} = \Psi^{(m)}(\Phi^{(m)})^{-1}\hat{\mathbf{y}}_i^{(m)} \tag{7}$$

where  $\Phi^{(m)}$  is the interference matrix of user  $m$ . LS criterion in (7) coincides with the maximum-likelihood (ML) estimation, since the noise is Gaussian.

If (I)DFTs in the algorithm described in the previous section are calculated using the (I)FFT algorithm, a great reduction in complexity is obtained compared to other iterative proposals. Therefore, we refer to this successive interference cancellation proposal as FFT-based interference cancellation (FFT-IC). In Sect. 3 we provide a particular upper-bound for the mean square symbol error at convergence for the compensation algorithm, exploiting the structure of the multicarrier systems uplink.

### 3 Mean Squared Symbol Error Analysis

In [9] is shown that if the SAGE algorithm is initialized in a region suitably close to a local maximum of the likelihood function, then the sequence of estimates will converge monotonically in norm to it. Besides this general property, in this section we analyze the convergence of the FFT-IC successive cancellation algorithm by studying the mean square error (MSE) of the compensated symbols as the number of iterations increases. Therefore, first we reformulate the update equation of  $\hat{\mathbf{s}}_{i+1}^{(m)}$  (7) in a more appropriate form for the convergence analysis. Then, we define the MSE per subcarrier of each user and we describe it as a vector difference equation in Lemma 1. Assuming that the MSE at every carrier of each user converges to similar values, we find an upper bound of the MSE for a large number of iterations and present it in Theorem 1.

#### 3.1 Reformulation of the Signal of Each User

Replacing  $\mathbf{y}$  by (3) in (6) and the result in (7), we obtain

$$\begin{aligned} \hat{\mathbf{s}}_{i+1}^{(m)} &= \Psi^{(m)}(\Phi^{(m)})^{-1} \left[ \Phi \mathbf{s} + \mathbf{z} - \Phi \left( \sum_{l=0}^{m-1} \hat{\mathbf{s}}_{i+1}^{(l)} + \sum_{l=m+1}^{K-1} \hat{\mathbf{s}}_i^{(l)} \right) \right] \\ &= \mathbf{s}^{(m)} + \Psi^{(m)}(\Phi^{(m)})^{-1} \Phi \left[ \sum_{l=0}^{m-1} (\mathbf{s}^{(l)} - \hat{\mathbf{s}}_{i+1}^{(l)}) + \sum_{l=m+1}^{K-1} (\mathbf{s}^{(l)} - \hat{\mathbf{s}}_i^{(l)}) \right] + \Psi^{(m)} \tilde{\mathbf{z}} \end{aligned} \tag{8}$$

where  $\tilde{\mathbf{z}} = (\Phi^{(m)})^{-1} \mathbf{z}$  is a Gaussian vector statistically equivalent to  $\mathbf{z}$ . In the second expression of (8) we used the fact that  $\mathbf{s} = \sum_{m=0}^{K-1} \mathbf{s}^{(m)}$  and  $\mathbf{s}^{(m)} = \Psi^{(m)}(\Phi^{(m)})^{-1} \Phi \mathbf{s}^{(m)}$ . Note that (8) expresses the update  $\hat{\mathbf{s}}_{i+1}^{(m)}$  as a function of the true and estimated values of previous iterations. The estimation of the complete block is obtained computing the update  $\hat{\mathbf{s}}_{i+1}^{(m)}$  sequentially for every user and several iterations. The Eq. (8) is useful to study the mean square symbol error performance at each iteration of the compensation method, as discussed in the next subsection.

To avoid the mix of updated and non-updated vectors in Eq. (8), we introduce the indexation  $q = iK + m$ , with  $0 \leq m \leq K - 1$  and  $i = 0, 1, \dots, I - 1$ , that selects the information of the user  $m$  at iteration  $i$  employing a single index. In other words, the indexation

$q$  selects the users sequentially, through the iterations, in the same way that the successive cancellation criterion. The new indexation, in an example for SCAS, is depicted in Fig. 1. Using the new indexation, we can rewrite (8) as

$$\hat{s}_{q+1} = s_{|q+1|_K} + \Psi^{|q+1|_K} \sum_{l=q-K+2}^q (\Phi^{|q+1|_K})^{-1} \Phi(s_l - \hat{s}_l) + \Psi^{|q+1|_K} \tilde{z} \tag{9}$$

where  $|\cdot|_K$  is the module- $K$  operation and the vector indexation  $\mathbf{x}_q = \mathbf{x}_i^{(m)}$  corresponds to the relation  $q = iK + m$ . Noting that  $\Phi(\hat{s}_l - s_l) = \Phi^{l|_K}(\hat{s}_l - s_l)$  (since the non-zero elements in  $(\hat{s}_l - s_l)$  take the same elements from  $\Phi$  and  $\Phi^{l|_K}$ ) and that  $\Phi^{l|_K}$  is circulant, (9) can be written as

$$\hat{s}_{q+1} = s_{|q+1|_K} + \Psi^{|q+1|_K} \sum_{l=q-K+2}^q A(l, q+1)(s_l - \hat{s}_l) + \Psi^{|q+1|_K} \tilde{z} \tag{10}$$

where  $A(l, q+1) = (\Phi^{|q+1|_K})^{-1} \Phi^{l|_K} = \mathbf{F}_{N_c} (\mathbf{D}^{(q+1)})^{-1} \mathbf{D}^{(l)} \mathbf{F}_{N_c}^H$  is a circulant matrix, and  $(\mathbf{D}^{(q+1)})^{-1} \mathbf{D}^{(l)} = \text{diag}\{1, e^{j2\pi(\xi^{l|_K} - \xi^{q+1|_K})/N_c}, \dots, e^{j2\pi(\xi^{l|_K} - \xi^{q+1|_K})(N_c-1)/N_c}\}$ .

### 3.2 Mean Square Symbol Error

The mean square symbol error (MSE) of  $\hat{s}_{q+1}$  at subcarrier  $n$  conditioned to the knowledge of  $\hat{s}_l$  for  $q - K + 2 \leq l \leq q$ , where  $n$  is allocated to user  $(|q+1|_K)$ , is defined by

$$[\mathbf{m}_{q+1}]_n = \text{MSE}\{[\hat{s}_{q+1}]_n | \hat{s} : q - K + 2 \leq l \leq q\} = \text{E}\left\{ |[\hat{s}_{q+1}]_n - [s_{|q+1|_K}]_n|^2 \right\} \tag{11}$$

where  $[\mathbf{x}]_n$  selects the  $n$ th element of  $\mathbf{x}$ . Considering this definition, we introduce the following lemma.

**Lemma 1** *The MSE  $\mathbf{m}_{q+1}$  at subcarrier  $n$  is bounded by a linear combination of the MSEs of previous iterations  $\{q - K + 2 \dots q\}$ , as follows*

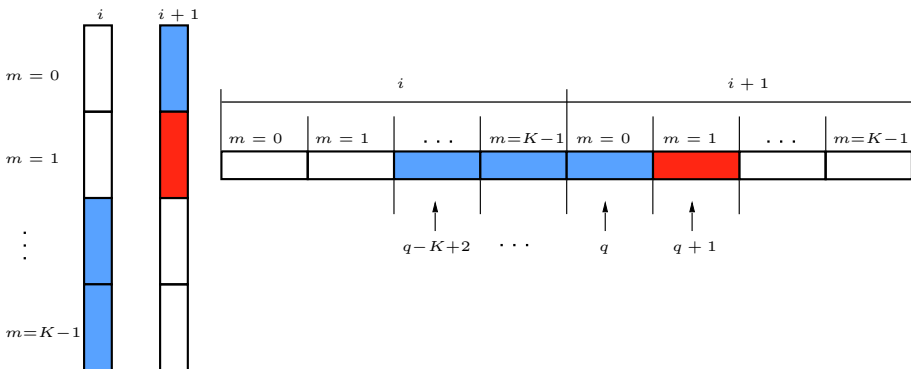


**Fig. 1** Representation of the indexation  $q = iK + m$ . Blue denotes previous users whereas red represents the user to be updated. (Color figure online)

$$[\mathbf{m}_{q+1}]_n \leq (K - 1)(2N_h + 1) \sum_{l=q-K+2}^q [\mathbf{C}_{l,q+1} \mathbf{m}_l]_n + \sigma^2 \tag{12}$$

where matrix  $\mathbf{C}_{l,q+1}$  weights the interference that the user  $|l|_K$  introduces to the user  $|q + 1|_K$ , with elements

$$[\mathbf{C}_{l,q+1}]_{n,p} = \begin{cases} |a_{l,q+1}(|n - p|_{N_c})|^2 & \text{if } 0 \leq n \leq N_c - 1 \text{ and } -N_h \leq p \leq N_h \\ 0 & \text{otherwise} \end{cases} \tag{13}$$

where

$$a_{l,q+1}(n) = \text{IDFT}\{1, e^{j2\pi(\xi^{||k} - \xi^{||q+1|_k})/N_c}, \dots, e^{j2\pi(\xi^{||l} - \xi^{||q+1|_k})(N_c-1)/N_c}\} \tag{14}$$

and  $N_h$  is chosen to consider more than 99.9 % of the interference energy that a carrier produces into its neighbors (more details in Appendix 1).

*Proof* The proof is included in Appendix 1. □

Lemma 1 is used to obtain an upper-bound for the MSE per subcarrier at convergence, i.e. when the number of iterations is large. The result is stated in the theorem below.

**Theorem 1** *If the sum of the MSE of each user  $\sum_{q=i}^{i+K-1} \mathbf{m}_{q+1}$  converges to a mean  $\bar{\mathbf{m}}_\infty$  for  $i \rightarrow \infty$ , and all its elements are equal, i.e.  $[\bar{\mathbf{m}}_\infty]_n = \zeta$ , for  $0 \leq n \leq N_c - 1$ ; the MSE per subcarrier at convergence is upper-bounded by*

$$\zeta \leq \frac{N_a \sigma^2}{N_a - (K - 1)(2N_h + 1)C_{sum}} \tag{15}$$

where  $C_{sum} = \sum_{n=0}^{N_c-1} \sum_{l=0}^{N_c-1} [\bar{\mathbf{C}}]_{n,l}$  and  $\bar{\mathbf{C}} = \sum_{q=0}^{K-1} \sum_{l=0, l \neq q}^{K-1} \Psi^{|q+1|_K} \mathbf{C}_{l,q+1} \Psi^{|l|_K}$ .

*Proof* From (12) and considering again the matrix  $\Psi^{|q+1|_K}$ , we can write the sum of the MSE of each carrier of each user as follows

$$\mathbf{1}^T \sum_{q=i}^{i+K-1} \Psi^{|q+1|_K} \mathbf{m}_{q+1} \leq (K - 1)(2N_h + 1) \mathbf{1}^T \sum_{q=i}^{i+K-1} \sum_{l=q-K+2}^q \Psi^{|q+1|_K} \mathbf{C}_{l,q+1} \mathbf{m}_l + N_a \sigma^2 \tag{16}$$

If the sum of the MSE of each user  $\sum_{q=i}^{i+K-1} \mathbf{m}_{q+1}$  converges to a mean vector  $\bar{\mathbf{m}}_\infty$  for  $i \rightarrow \infty$ , we can simplify (16) as

$$\begin{aligned} \mathbf{1}^T \bar{\mathbf{m}}_\infty &= \mathbf{1}^T \sum_{q=i}^{i+K-1} \Psi^{|q+1|_K} \mathbf{m}_{q+1} \leq (K - 1)(2N_h + 1) \\ &\quad \times \mathbf{1}^T \left[ \sum_{q=i}^{i+K-1} \sum_{l=q-K+2}^q \Psi^{|q+1|_K} \mathbf{C}_{l,q+1} \Psi^{|l|_K} \right] \bar{\mathbf{m}}_\infty + N_a \sigma^2 \\ \mathbf{1}^T \bar{\mathbf{m}}_\infty &\leq (K - 1)(2N_h + 1) \mathbf{1}^T \bar{\mathbf{C}} \bar{\mathbf{m}}_\infty + N_a \sigma^2 \end{aligned} \tag{17}$$

where  $\bar{\mathbf{C}} = \sum_{q=0}^{K-1} \sum_{l=0, l \neq q}^{K-1} \Psi^{|q+1|_K} \mathbf{C}_{l,q+1} \Psi^{|l|_K}$ . Note that  $\bar{\mathbf{C}}$  does not depend on  $i$  since it has period  $K$ .

Additionally, if the residual MSE at each carrier, denoted  $\zeta$ , is the same; we can solve the multiplication as  $\mathbf{1}^T \bar{\mathbf{C}} \bar{\mathbf{m}}_\infty = \zeta C_{sum}$ , where  $C_{sum} = \sum_{n=0}^{N_c-1} \sum_{l=0}^{N_c-1} [\bar{\mathbf{C}}]_{n,l}$ . Note that this assumption is realistic since the CFO is not correlated with user data and the channel effects are included in  $\mathbf{s}^{(m)}$ . Then, from (17) we can derive an *upper bound* for  $\zeta$  as follows

$$N_a \zeta \leq (K - 1)(2N_h + 1)\zeta C_{sum} + N_a \sigma^2 \tag{18}$$

$$\zeta \leq \frac{N_a \sigma^2}{N_a - (K - 1)(2N_h + 1)C_{sum}} \tag{19}$$

□

### 3.3 Additional Comments and Remarks

From (19) we note that if there is no CFO interference,  $C_{sum} = 0$ , and the MSE reaches the floor produced by the noise and it can be considered as the *lower performance bound*. On the other hand, (19) is valid as long as  $N_a - (K - 1)(2N_h + 1)C_{sum} > 0$ , then

$$C_{sum}(2N_h + 1) < \frac{N_a}{(K - 1)} \tag{20}$$

In Appendix 2 is shown that the largest value of  $C_{sum}$  is  $KN_t$ , however a set of simulations show that the averaged value is much less. In Fig. 2 we simulate the probability density function (pdf) of  $C_{sum}$  for a system with  $N_c = 1024$ ,  $K = 4$ , uniform CFO, and considering SCAS and ICAS ( $N_t = 20$  and  $L_t = 12$ ). In Fig. 2a we use  $|\zeta^{(m)}| < 0.3$ , whereas in Fig. 2b  $|\zeta^{(m)}| < 0.5$ . As expected,  $C_{sum}$  depends on the user allocation and CFO range. It is possible to verify in Fig. 2b that the probability that  $C_{sum}$  reaches the maximum value  $KN_t$  (4 for SCAS and 80 for ICAS) is very low. On the other hand, it should be noted that  $C_{sum}$  gives an idea of the interference that the CAS and CFO range introduce to the system.

Considering that  $N_h = 5$  collects most of the energy of the interference for any CFO value (see Appendix 1 for details) and that  $C_{sum}$  averaged value for  $|\zeta^{(m)}| < 0.3$  and ICAS is 15.89, (20) reduces to  $175 \lesssim \frac{N_a}{(K-1)}$ . Just as an example, it is easy to verify that the bound

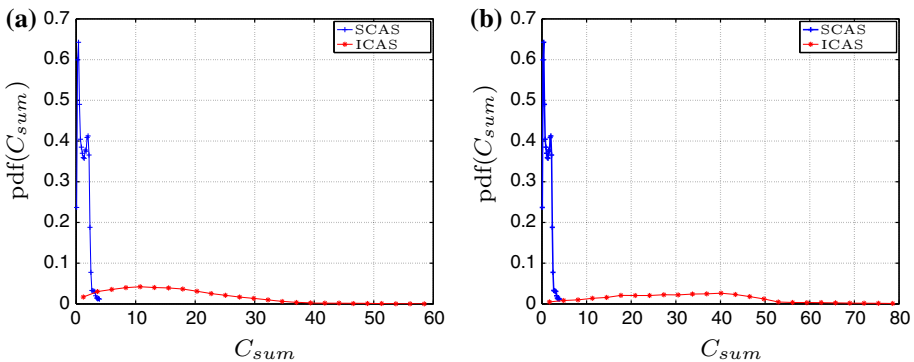


**Fig. 2** Probability density function of  $C_{sum}$  for a system with  $N_c = 1024$ ,  $K = 4$ , for SCAS and ICAS ( $N_t = 20$  and  $L_t = 12$ ), considering **a** CFO  $|\zeta^{(m)}| < 0.3$  and **b** CFO  $|\zeta^{(m)}| < 0.5$

results valid for an LTE system with ICAS,  $K = 4$  users and  $N_c = 1024$  subcarriers. In Sect. 4 we evaluate numerically the theoretical expression (12) and verify the accuracy of the bound (15) under different interference scenarios.

### 4 Numerical Simulations

In this section, we evaluate the mean square error (MSE) of the FFT-IC algorithm as a function of the iterations and compare it with the theoretical approximation and the upper-bound derived in Sect. 3.2. Additionally, we include some bit error rate (BER) curves for FFT-IC, Direct [15], and conjugate gradient (CG) [8].

For the simulations we consider a 3GPP LTE-like system with the following parameters:  $N_c = 1024$  subcarriers, sample frequency  $F_s = 15.36$  MHz, intercarrier spacing  $\Delta f = 15$  kHz, carrier frequency  $f_c = 2.5$  GHz, cyclic prefix  $N_{cp} = 152$ , and 16-QAM modulation. The OFDMA and SC-FDMA systems of  $K = 4$  users utilize a tile size of  $L_t = 12$  subcarriers, and  $N_t = 20$  tiles per user for GCAS (the users are allocated randomly among the tiles); or  $L_t = 240$  and  $N_t = 1$  for SCAS. The ITU Vehicular A channel with a speed of 50 km/h is employed [16]. The channel is considered known at the receiver and the symbols are recovered using a single-tap frequency domain equalizer. Although mathematically the CFO range can be  $|\zeta^{(m)}| < 0.5$ , we employ a range  $|\zeta^{(m)}| < 0.3$  since it is more realistic. If we assume that each user synchronizes with the BS in the downlink, the residual CFO is only due to Doppler shift. Considering LTE parameters [12] and a high speed train scenario [17], where the speed is 350 km/h, the Doppler shift leads to a CFO of 0.1.

In Fig. 3 we compare the BER for LS. For SCAS, all compensation algorithms converge to the Direct compensation since this allocation scheme does not introduce a significant amount of interference. Note that the averaged value of  $C_{sum}$  for this case is only 0.6. On the other hand, for GCAS the  $C_{sum}$  averaged value is 11.94, which means the interference is considerable and the compensation properties of the algorithms are brought to light. From the figure, it is clear that FFT-IC attains a similar BER than CG, but with a lower implementation complexity [10].

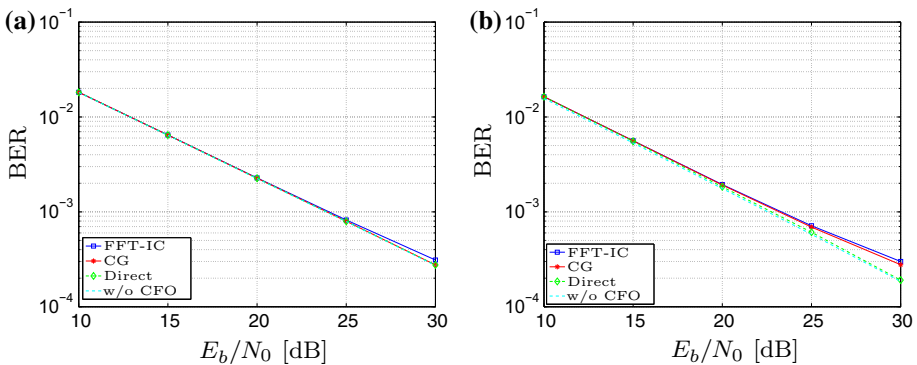


**Fig. 3** BER performance comparison between different CFO compensation methods for OFDMA, considering **a** SCAS and **b** GCAS for LS. The curves are obtained using the ITU Vehicular A channel and a CFO uniformly distributed in the interval  $|\zeta^{(m)}| < 0.3$

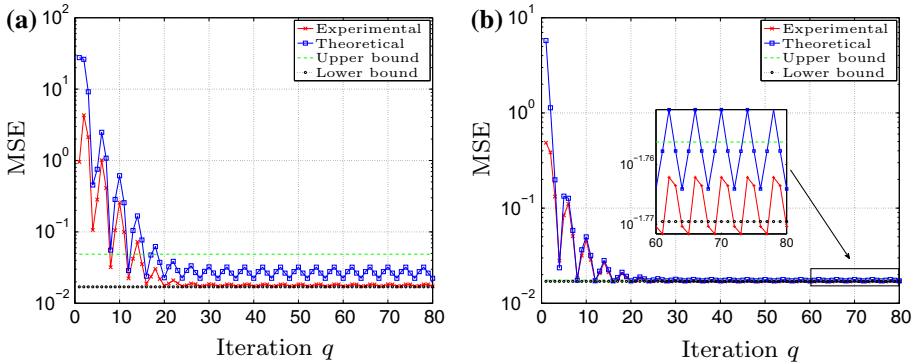


**Fig. 4** Learning curves of the proposed algorithm for an OFDMA system, with **a** GCAS and **b** SCAS. The curves are obtained considering a fixed CFO for every user ( $\xi^{(0)} = -0.1$ ,  $\xi^{(1)} = 0.2$ ,  $\xi^{(2)} = -0.15$ , and  $\xi^{(3)} = 0.05$ ) and  $\sigma^2 = 0.001$

The Fig. 4 depicts the results of the convergence analysis of Sect. 3 for an OFDMA system with GCAS and SCAS considering a fixed CFO for every user ( $\xi^{(0)} = -0.1$ ,  $\xi^{(1)} = 0.2$ ,  $\xi^{(2)} = -0.15$ , and  $\xi^{(3)} = 0.05$ ) and  $\sigma^2 = 0.001$ . The figure considers the experimental MSE at iteration  $q$  from (11), the theoretical MSE from (12) (both calculated as  $\sum_{n=0}^{N_c-1} [\mathbf{m}_q]_n$ ), the upper bound (15) (calculated as  $N_K \xi$ ), and the lower bound  $N_K \sigma^2$ . From the figure we note that the theoretical MSE is accurate for both CASs and that the experimental and theoretical MSE curves lie in average between the lower and the upper bounds, as expected. On the other hand, the upper bound is tighter for systems with low interference, as is the case of SCAS in Fig. 4b. The average of  $C_{sum}$  for  $|\xi^{(m)}| < 0.3$  is approximately 0.60 for SCAS and 11.94 for GCAS, then the condition (20) is verified in both cases: for SCAS we have  $6.6 \approx C_{sum}(2N_h + 1) < \frac{N_a}{(K-1)} = 320$ , whereas for GCAS  $131.34 \approx C_{sum}(2N_h + 1) < \frac{N_a}{(K-1)} = 320$ .

### 5 Conclusion

In this work we analyze the carrier frequency offset (CFO) compensation performance of efficient successive cancellation algorithms, for the uplink of multicarrier systems. We derive a useful upper-bound for the mean square error at convergence that is tight for systems with moderate interference. Additionally, the bound gives an idea of the level of interference produced by the CFO and the user carrier allocation scheme. On the other hand, this study complements the general convergence results for the space-alternating generalized expectation-maximization algorithm when is applied for CFO compensation.

### Appendix 1: Proof of Lemma 1

*Proof* By replacing  $\hat{s}_{q+1}$  by (10), we can rewrite (11) as

$$\begin{aligned}
 [\mathbf{m}_{q+1}]_n &= \text{MSE}\{\hat{\mathbf{s}}_{q+1}_n | \hat{\mathbf{s}}_l : q - K + 2 \leq l \leq q\} \\
 &= \text{E} \left\{ \left| \sum_{l=q-K+2}^q [\mathbf{A}(l, q + 1)(\mathbf{s}_l - \hat{\mathbf{s}}_l)]_n + [\tilde{\mathbf{z}}]_n \right|^2 \right\} \tag{21}
 \end{aligned}$$

Note that  $\Psi^{l|q+1|_K}$  is not necessary due to the selection operation  $[\cdot]_n$ .

Since the noise is independent of the transmitted data and has zero mean, (21) can be written as in the following expression

$$[\mathbf{m}_{q+1}]_n = \text{E} \left\{ \left| \sum_{l=q-K+2}^q [\mathbf{A}(l, q + 1)(\mathbf{s}_l - \hat{\mathbf{s}}_l)]_n \right|^2 \right\} + \sigma^2 \tag{22}$$

Using the Cauchy–Schwarz inequality in (22), the equation can be rewritten as

$$[\mathbf{m}_{q+1}]_n \leq (K - 1) \sum_{l=q-K+2}^q \text{E} \left\{ \left| [\mathbf{A}(l, q + 1)(\mathbf{s}_l - \hat{\mathbf{s}}_l)]_n \right|^2 \right\} + \sigma^2 \tag{23}$$

By defining

$$e_l(n) = [(\mathbf{s}_l - \hat{\mathbf{s}}_l)]_n, \text{ and} \tag{24}$$

$$a_{l,q+1}(n) = \text{IDFT} \{ 1, e^{j2\pi(\xi^{ll}_K - \xi^{lq+1|_K})/N_c}, \dots, e^{j2\pi(\xi^{ll} - \xi^{lq+1})/N_c} \} \tag{25}$$

(first column of  $\mathbf{A}(l, q + 1)$ ) and considering  $n$  is allocated to user  $|q + 1|_K$ , we can express the circular matrix multiplication of (23) as the following circular convolution

$$[\mathbf{m}_{q+1}]_n \leq (K - 1) \sum_{l=q-K+2}^q \text{E} \left\{ \left| \sum_{p=0}^{N_c-1} a_{l,q+1}(|n - p|_{N_c}) e_l(p) \right|^2 \right\} + \sigma^2 \tag{26}$$

As the energy of the interference is located close to  $n$ , we consider only  $N_h$  carriers adjacent to  $n$ , where  $N_h$  is chosen to consider more than 99.9 % of the interference energy. Then, applying again the Cauchy–Schwarz inequality and assuming that the CFO is deterministic and unknown, and  $n$  is allocated to user  $|q + 1|_K$ , (26) can be rewritten as

$$[\mathbf{m}_{q+1}]_n \leq (K - 1)(2N_h + 1) \sum_{l=q-K+2}^q \sum_{p=-N_h}^{N_h} |a_{l,q+1}(|n - p|_{N_c})|^2 [\mathbf{m}_l]_{|n-p|_{N_c}} + \sigma^2 \tag{27}$$

where it is used that  $\text{E}\{|e_l(n)|^2\} = [\mathbf{m}_l]_n$ . If we define the  $N_c \times N_c$  banded convolution matrix  $\mathbf{C}_{l,q+1}$ , with elements

$$[\mathbf{C}_{l,q+1}]_{n,p} = \begin{cases} |a_{l,q+1}(|n - p|_{N_c})|^2 & \text{if } 0 \leq n \leq N_c - 1 \text{ and } -N_h \leq p \leq N_h \\ 0 & \text{otherwise} \end{cases} \tag{28}$$

the MSE as a function of the previous iterations results

$$[\mathbf{m}_{q+1}]_n \leq (K - 1)(2N_h + 1) \sum_{l=q-K+2}^q [\mathbf{C}_{l,q+1} \mathbf{m}_l]_n + \sigma^2 \tag{29}$$

□

## Appendix 2: Maximum Value of $C_{sum}$

The maximum value of  $C_{sum}$  is produced by a system with ICAS, where contiguous tiles belong to users with opposed CFO values, i.e.  $\xi^{(m_1)} = -\xi^{(m_2)}$ , if  $m_1$  and  $m_2$  are contiguous users. On the other hand, the maximum value of CFO that results in full-rank  $\Phi$  matrices is  $|\xi^{(m)}| < 0.5$  [15].

Considering the worst case  $|\xi^{(m)}| = 0.5$ , and that  $\xi^{(1)} = -0.5$  (the CFO of the user allocated in the first tile is  $-0.5$ ),<sup>1</sup> the matrix  $\tilde{C}$  has the following structure

$$\tilde{C} = \begin{pmatrix} \tilde{C}_{0,0} & \tilde{C}_{0,1} & \cdots & \tilde{C}_{0,N_t-1} \\ \tilde{C}_{1,0} & \tilde{C}_{1,1} & \cdots & \tilde{C}_{1,N_t-1} \\ \vdots & & \ddots & \vdots \\ \tilde{C}_{N_t-1,0} & \tilde{C}_{N_t-1,1} & \cdots & \tilde{C}_{N_t-1,N_t-1} \end{pmatrix} \tag{30}$$

where the only non zero matrices are  $\tilde{C}_a = \tilde{C}_{1,0} = \tilde{C}_{3,2} = \cdots = \tilde{C}_{N_t-1,N_t-2}$  and  $\tilde{C}_b = \tilde{C}_{0,1} = \tilde{C}_{2,3} = \cdots = \tilde{C}_{N_t-2,N_t-1}$ , with dimension  $L_t \times L_t$ ; and values

$$\tilde{C}_a = \begin{pmatrix} 0 & 0 & \cdots & 1 \\ 0 & 0 & \cdots & 0 \\ \vdots & \vdots & \ddots & \vdots \\ 0 & 0 & \cdots & 0 \end{pmatrix} \tag{31}$$

$$\tilde{C}_b = \begin{pmatrix} 0 & 0 & \cdots & 0 \\ 0 & 0 & \cdots & 0 \\ \vdots & \vdots & \ddots & \vdots \\ 1 & 0 & \cdots & 0 \end{pmatrix} \tag{32}$$

As in each column or row of (30) there is either one  $\tilde{C}_a$  or one  $\tilde{C}_b$ , it is easy to see that the worst-case value results  $C_{sum} = KN_t$ .

## References

1. Holma, H., & Toskala, A. (2009). *LTE for UMTS–OFDMA and SC-FDMA based radio access* (1st ed.). New York: Wiley.
2. 3rd generation partnership project (3GPP) technical specification group radio access network; physical layer aspects for evolved universal terrestrial radio access (UTRA) (release 7). *3GPP TR 25.814, V7.1.0* (Sept. 2006).
3. Pun, M.-O., Morelli, M., & Jay Kuo, C. C. (2007). *Multi-carrier techniques for broadband wireless communications: A signal processing perspectives*. London: Imperial College Press.
4. Nguyen, H., de Carvalho, E., & Prasad, R. (2010). Joint estimation of the timing and frequency offset for uplink OFDMA. *Wireless Personal Communications*, 52(1), 119–131.
5. Lee, K., Moon, S.-H., Lee, S.-R., & Lee, I. (2012). Low complexity pilot assisted carrier frequency offset estimation for OFDMA uplink systems. *IEEE Transactions on Wireless Communications*, 11(8), 2690–2695.

<sup>1</sup> If  $\xi^{(1)} = 0.5$ , the worst case results  $C_{sum} = N_t - 2$ .

6. An, C., & Ryu, H.-G. (2015). A novel CFO suppression algorithm for OFDMA uplink communication system. *Wireless Personal Communications*, 80(1), 357–368.
7. Hsu, C.-Y., & Wu, W.-R. (2008). A low-complexity zero-forcing CFO compensation scheme for OFDMA uplink systems. *IEEE Trans. Wireless Commun.*, 7(10), 3657–3661.
8. Lee, K., Lee, S.-R., Moon, S.-H.-, & Lee, I. (2012). MMSE-based CFO compensation for uplink OFDMA systems with conjugate gradient. *IEEE Transactions on Wireless Communications*, 11(8), 2767–2775.
9. Fessler, J. A., & Hero, A. O. (1994). Space-alternating generalized expectation-maximization algorithm. *IEEE Transactions on Signal Processing*, 42(10), 2664–2677.
10. Bai, L., & Yin, Q. (2012). Frequency synchronization for the OFDMA uplink based on the tile structure of IEEE 802.16e. *IEEE Transactions on Vehicular Technology*, 61(5), 2348–2353.
11. Dempster, A. P., Laird, N. M., & Rubin, D. B. (1977). Maximum likelihood from incomplete data via the EM algorithm. *Journal of the Royal Statistical Society, Series B*, 39(1), 1–38.
12. Dahlman, E., Parkvall, S., Sköld, J., & Beming, P. (2008). *3G evolution HSPA and LTE for mobile broadband* (2nd ed.). Amsterdam: Elsevier.
13. IEEE standard for local and metropolitan area networks part 16: Air interface for fixed broadband wireless access systems. In *IEEE Std 802.16-2004 (Revision of IEEE Std 802.16-2001)* (pp. 01–857) (2004).
14. Barbarossa, S., Pompili, M., & Giannakis, G. B. (2002). Channel-independent synchronization of orthogonal frequency division multiple access systems. *IEEE Journal on Selected Areas in Communications*, 20(2), 474–486.
15. Cao, Z., Tureli, U., & Yao, Y.-D. (2007). Low-complexity orthogonal spectral signal construction for generalized OFDMA uplink with frequency synchronization errors. *IEEE Transactions on Vehicular Technology*, 56(3), 1143–1154.
16. ITU-R. (1997). Guidelines for evaluation of radio transmission technologies for IMT-2000. In *Recommendation ITUR M1225* (Vol. 93, no. 3, pp. 148–56).
17. LTE. (July 2012). Evolved universal terrestrial radio access (E-UTRA); base station (BS) radio transmission and reception.



**Gustavo J. González** was born in Bahía Blanca, Argentina. He received the B.Sc. degree in 2007, and the Ph.D. degree in 2012 from Universidad Nacional del Sur (UNS), Bahía Blanca, Argentina. In 2007, he joined the undergraduate Department of Electrical and Computer Engineering at UNS. He is researcher of the Consejo Nacional de Investigaciones Científicas y Técnicas (CONICET) since 2014. His research interests include digital signal processing for wireless communications, in particular frequency synchronization, OFDM/A, filter bank multicarrier, and full-duplex systems.



**Fernando H. Gregorio** is from Bahía Blanca, Argentina. He received the B.Sc. degree from the Universidad Tecnológica Nacional (UTN), Bahía Blanca, Argentina in 1999, the M.Sc. degree in electrical engineering from the Universidad Nacional del Sur (UNS), Bahía Blanca in 2003 and the D.Sc. (electrical engineering) degree from the Signal Processing Laboratory, Helsinki University of Technology (TKK), Espoo, Finland, in 2007. He is currently a professor in the Department of Electrical and Computer Engineering at UNS and researcher of the Consejo Nacional de Investigaciones Científicas y Técnicas (CONICET) of Argentina. His research interests include radio frequency impairments in MIMO-OFDM systems and multiuser communications.



**Juan E. Cousseau** was born in Mar del Plata, Argentina. He received the B.Sc. from the Universidad Nacional del Sur (UNS), Bahía Blanca, Argentina, in 1983, the M.Sc. degree from COPPE/Universidade Federal do Rio de Janeiro (UFRJ), Brazil, in 1989, and the Ph.D. from COPPE/UFRJ, in 1993, all in electrical engineering. Since 1984, he has been with the undergraduate Department of Electrical and Computer Engineering at UNS. He has also been with the graduate Program at the same university since 1994. He is a Senior researcher of the Consejo Nacional de Investigaciones.



**Carlos H. Muravchik** (S'81-M'83-SM'99) graduated as an Electronics Engineer from the National University of La Plata, Argentina, in 1973. He received the M.Sc. in Statistics (1983) and the M.Sc. (1980) and Ph.D. (1983) degrees in Electrical Engineering, from Stanford University, Stanford, CA. He is a Professor at the Department of the Electrical Engineering of the National University of La Plata and chairman of its Industrial Electronics, Control and Instrumentation Laboratory (LEICI). He is also a member of the Comisión de Investigaciones Científicas de la Pcia. de Buenos Aires. He was a Visiting Professor to Yale University in 1983 and 1994, to the University of Illinois at Chicago in 1996, 1997, 1999 and 2003 and to Washington University in St Louis in 2006 and 2010. Since 1999 he is a member of the Advisory Board of the journal *Latin American Applied Research* and was an Associate Editor of the *IEEE Transactions on Signal Processing* (2003–2006). His research interests are in the area of statistical and array signal processing with biomedical, communications and control applications, and in nonlinear control systems.